3-Dimmensional PML Absorbing Boundary Condition for Dispersive and Anisotropic Medium

Hiroyasu Sato, Qiang Chen, and Kunio Sawaya
Department of Electrical and Communication Engineering,
Tohoku University, Aoba-ku, Sendai, 980-8579, Japan

1. Introduction

As an efficient absorbing boundary condition for the FDTD method, PML(Perfectly Matched Layer) has been proposed by Berenger[1] and contributed to the improvement of accuracy and reliability of FDTD in the open radiation problem. Berenger's PML has been devised for the case in which the analysis region is free space. The usual absorbing boundary condition (ABC), such as the Mur-ABC [2] and the Higdon-ABC [3]. is invalid when the analysis region is filled with dispersive and anisotropic medium, such as the magnetoplasma. Recently, it has been demonstrated that the PML is applicable for lossy medium[4], dispersive medium [5], anisotropic medium [6]. However, the 3-D analysis for the medium which is both dispersive and anisotropic has not been carried out.

In this paper, a PML-based absorbing boundary condition for the dispersive and anisotropic medium is proposed. While Berenger deduced PML which is matched to the impedance of free space, we derive dispersive and anisotropic PML which is matched to the impedance of the uniaxially anisotropic medium. In order to demonstrate the validity of the proposed boundary condition, numerical results for dispersive and anisotropic medium including some type of dispersion in tensor permittivity are presented.

2. Formulation

In the dispersive and anisotropic PML medium, Maxwell's equation is devided into the 12 partial differential equation as follows.

$$\frac{\partial D_{xy}}{\partial t}+\frac{\sigma_y^D}{\varepsilon_0}D_{xy} = \frac{\partial(H_{zx}+H_{zy})}{\partial y},\quad \frac{\partial D_{xz}}{\partial t}+\frac{\sigma_z^D}{\varepsilon_0}D_{xz}=-\frac{\partial(H_{yx}+H_{yz})}{\partial z} \tag{1-a}$$

$$\frac{\partial D_{yx}}{\partial t}+\frac{\sigma_x^D}{\varepsilon_0}D_{yx} = \frac{\partial(H_{xy}+H_{xz})}{\partial z},\quad \frac{\partial D_{yz}}{\partial t}+\frac{\sigma_z^D}{\varepsilon_0}D_{yz}=-\frac{\partial(H_{zx}+H_{zy})}{\partial x} \tag{1-b}$$

$$\frac{\partial D_{zx}}{\partial t}+\frac{\sigma_x^D}{\varepsilon_0}D_{zx} = \frac{\partial(H_{yx}+H_{yz})}{\partial x},\quad \frac{\partial D_{zy}}{\partial t}+\frac{\sigma_y^D}{\varepsilon_0}D_{zy}=-\frac{\partial(H_{xy}+H_{xz})}{\partial y} \tag{1-c}$$

$$\mu_0\frac{\partial H_{xy}}{\partial t}+\sigma_y^* H_{xy} = -\frac{\partial E_z}{\partial y},\quad \mu_0\frac{\partial H_{xz}}{\partial t}+\sigma_z^* H_{xz}=\frac{\partial E_y}{\partial z} \tag{1-d}$$

$$\mu_0\frac{\partial H_{yx}}{\partial t}+\sigma_x^* H_{yx} = -\frac{\partial E_x}{\partial z},\quad \mu_0\frac{\partial H_{yz}}{\partial t}+\sigma_z^* H_{yz}=\frac{\partial E_z}{\partial x} \tag{1-e}$$

$$\mu_0\frac{\partial H_{zx}}{\partial t}+\sigma_x^* H_{zx} = -\frac{\partial E_y}{\partial x},\quad \mu_0\frac{\partial H_{zy}}{\partial t}+\sigma_y^* H_{zy}=\frac{\partial E_x}{\partial y} \tag{1-f}$$

where $(\sigma_x^D,\sigma_y^D,\sigma_z^D,\sigma_x^*,\sigma_y^*,\sigma_z^*)$ are the electric conductivity and the magnetic conductivity to absorb the plane wave composed of electric flux density $\boldsymbol{D}$ and magnetic field $\boldsymbol{H}$, respectively. $\boldsymbol{D},\boldsymbol{H}$ are splitted as follows.

$$D_x = D_{xy}+D_{xz},\quad D_y=D_{yx}+D_{yz},\quad D_z=D_{zx}+D_{zy} \tag{2-a}$$

$$H_x = H_{xy}+H_{xz},\quad H_y=H_{yx}+H_{yz},\quad H_z=H_{zx}+H_{zy} \tag{2-b}$$

Relations between $\boldsymbol{D}$ and $\boldsymbol{E}$ are given by

$$\boldsymbol{D}(\omega) = \bar{\varepsilon}(\omega)\cdot\boldsymbol{E}(\omega) \quad (3\text{-a})$$

$$\bar{\varepsilon}(\omega) = \begin{pmatrix} \varepsilon_{xx}(\omega) & \varepsilon_{xy}(\omega) & \varepsilon_{xz}(\omega) \\ \varepsilon_{yx}(\omega) & \varepsilon_{yy}(\omega) & \varepsilon_{yz}(\omega) \\ \varepsilon_{zx}(\omega) & \varepsilon_{zy}(\omega) & \varepsilon_{zz}(\omega) \end{pmatrix} \quad (3\text{-b})$$

Next, a plane wave shown Fig.1 is considered. The field components for $\boldsymbol{D}$ and $\boldsymbol{H}$ are given by

$$D_{xy} = D_{xy0}e^{-j\omega(\xi x+\eta y+\zeta z-t)}, \quad D_{xz} = D_{xz0}e^{-j\omega(\xi x+\eta y+\zeta z-t)} \quad (4\text{-a})$$
$$D_{yx} = D_{yx0}e^{-j\omega(\xi x+\eta y+\zeta z-t)}, \quad D_{yz} = D_{xz0}e^{-j\omega(\xi x+\eta y+\zeta z-t)} \quad (4\text{-b})$$
$$D_{zx} = D_{zx0}e^{-j\omega(\xi x+\eta y+\zeta z-t)}, \quad D_{zy} = D_{zy0}e^{-j\omega(\xi x+\eta y+\zeta z-t)} \quad (4\text{-c})$$
$$H_{xy} = H_{xy0}e^{-j\omega(\xi x+\eta y+\zeta z-t)}, \quad H_{xz} = H_{xz0}e^{-j\omega(\xi x+\eta y+\zeta z-t)} \quad (4\text{-d})$$
$$H_{yx} = H_{yx0}e^{-j\omega(\xi x+\eta y+\zeta z-t)}, \quad H_{yz} = H_{yz0}e^{-j\omega(\xi x+\eta y+\zeta z-t)} \quad (4\text{-e})$$
$$H_{zx} = H_{zx0}e^{-j\omega(\xi x+\eta y+\zeta z-t)}, \quad H_{zy} = H_{zy0}e^{-j\omega(\xi x+\eta y+\zeta z-t)} \quad (4\text{-f})$$

where ξ, η, ζ are wave numbers correspond to x, y, z, respectively. Substituting eq.(4) into eq.(1), and imposing following matching conditions

$$\frac{\sigma_x^D}{\varepsilon_0} = \frac{\sigma_x^*}{\mu_0}, \quad \frac{\sigma_y^D}{\varepsilon_0} = \frac{\sigma_y^*}{\mu_0}, \quad \frac{\sigma_z^D}{\varepsilon_0} = \frac{\sigma_z^*}{\mu_0}, \quad (5)$$

the intrisic impedance $Z^D = D_0/H_0$ becomes the same to the analysis region.

3. Discretization for FDTD

The leap frog calculation is performed as $\boldsymbol{E} \Rightarrow \boldsymbol{H} \Rightarrow \boldsymbol{D} \Rightarrow (\boldsymbol{E})$ in turn. The discretization for $\boldsymbol{E} \Rightarrow \boldsymbol{H}$, $\boldsymbol{H} \Rightarrow \boldsymbol{D}$ is the same to the normal FDTD calculation. For $\boldsymbol{D} \Rightarrow (\boldsymbol{E})$ procedure, the relation $\boldsymbol{D} = \varepsilon_0\bar{\varepsilon}\cdot\boldsymbol{E}$ in frequency domain is transformed into time domain using Fourier transform because the medium is dispersive. As the method for evaluate $\boldsymbol{E}$ from $\boldsymbol{D}$, the auxialiary differential equation (ADE) method [7], and the recursive convolution (RC) method [8] are applicable and the ADE method is adopted in this report. The procedure of the derivation of discretized equation by the ADE method is omitted.

4. Numerical results In order to demonstrate the validity of the proposed boundary condition, numerical calculation for the dispersive and uniaxially anisotropic medium including Debye and Lorentz types of dispersion given by

$$\varepsilon_{xx}(\omega) = \varepsilon_{yy}(\omega) = \varepsilon_0\left[\varepsilon_\infty + \frac{(\varepsilon_s-\varepsilon_\infty)\omega_0^2}{\omega_0^2 + j2\omega\delta - \omega^2}\right] \quad (6)$$

$$\varepsilon_{zz}(\omega) = \varepsilon_0\left[\varepsilon_\infty + \frac{\varepsilon_s-\varepsilon_\infty}{1+j\frac{\omega}{\omega_0}}\right] \quad (7)$$

is performed, where ε_s and ε_∞ are permittivity at $\omega = 0$, $\omega \to \infty$, respectively, and ω_0 is the resonance angular frequency. δ is the dumping coefficient. Table 1 shows the parameters of the tensor permittivity.

Fig.2 shows the model for the calculation, where an electric dipole generating E_z is located at the center of analysis region and the exciting pulse is $p(t) = cos^6(\frac{\pi t}{\Delta})$, where $\Delta = 0.5ns$. Each cell size is 5.45cm, number of cells are $83\times83\times83$, and the time step Δt

is 0.1ns. The PML thickness is 16 cells. Fig.3 shows another model to obtain a reference solution, where a large analysis region Ω of $191 \times 191 \times 191$ cells surrounded by a perfectly conducting boundary is used. Fig.4 shows the time response of the electric field of the model shown in Fig.2 in the case with and without the PML. It can be pointed out that the numerical results using the proposed PML converge rapidly. Fig.5 shows the local error defined by

$$\text{Local error} = \frac{E_z^{PML} - E_z^{\Omega}}{E_z^{MAX}} \tag{8}$$

where E_z^{MAX} is maximum value and E_z^{Ω} is the reference solution obtained by using the model of Fig.3. The local error is less than -80dB and the validity of the proposed PML is demonstrated.

4. Conclusion PML-based absorbing boundary condition for dispersive and anisotropic medium has been proposed. Numerical results have shown that the proposed absorbing boundary condition can be matched the impedance of uniaxially anisotropic medium composed by Debye and Lorentz type dispersion.

References

[1] J.P. Berenger: "A perfectly matched layer for the absorption of electromagnetic waves", Journal of Computational Phisics, **114**, 1, pp.185-200 (1994).
[2] G. Mur: "Absorbing boundary conditions for the finite-difference approximation of the time-domain electromagnetic-field equation", IEEE Trans. Electromagn. Compat., **EMC-23**, 4, pp.377-382 (1981).
[3] R.L. Higdon: "Absorbing boundary condition for difference approximations to the multi-dimensional wave equation", Mathematics of Computation, **47**, 176, pp.437-459 (1986).
[4] J. Fang, Z. Wu: "Generalized perfectly matched layer – An extension of Berenger's perfectly matched layer boundary condition", IEEE Microwave Guided. Lett., **5**, 12, pp.451-453 (1995).
[5] T.Uno: "Perfectly Matched Layer Absorbing Boundary Condition for Dispersive Medium ", *IEEE Microwave Guided. Lett.*, vol. 7, no.9, pp. 264-266, (1997).
[6] S. G. Garcia, I. V. Perez, R. G. Martin, B. G. Olmedo, "Applicability of the PML absorbing boundary condition to dielectric anisotropic media", *Electronics Letters*, vol. 32, no. 14, pp. 1270-1271 (1996).
[7] T. Kashiwa, N.Yoshida and I. Fukai, "A Treatment by the finite-difference time-domain method of the dispersive characteristics associated with orientation polarization", *Trans. IEICE*, E73, no. 8, pp. 1326-1328, (1990).
[8] K. S. Kunz, R. J. Luebbers, "The Finite Difference Time Domain Method for Electromagnetics", Boca Raton, FL, CRC Press, (1993).

Table 1: Parameters of tensor permittivity

	ε_s	ε_∞	f_0[MHz]	δ
ε_{xx}(Lorentz)	4	2	300	100×10^6
ε_{yy}(Lorentz)	6	4	700	350×10^6
ε_{zz}(Debye)	10	2	200	

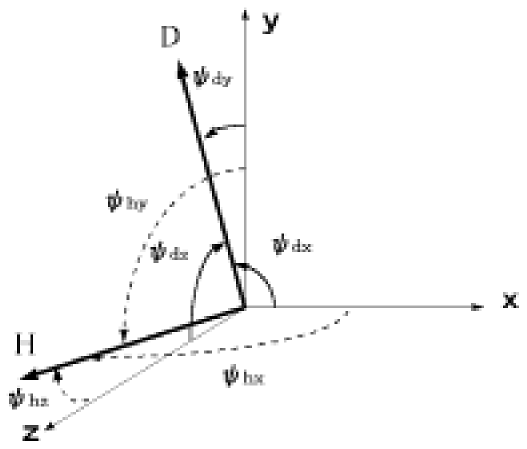

Figure 1: A plane wave in dispersive and anisotropic PML medium.

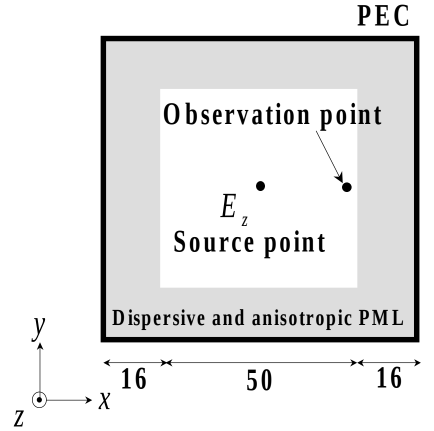

Figure 2: Model for calculation.

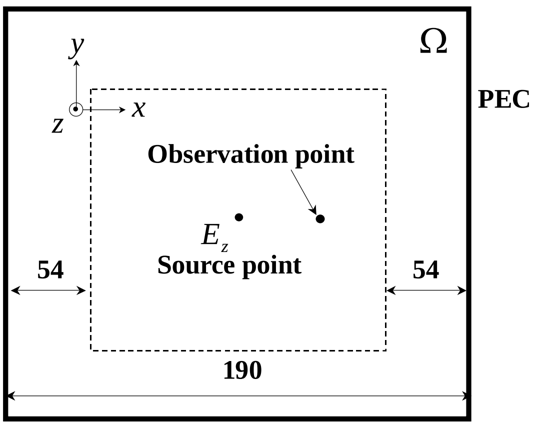

Figure 3: Large model to obtain reference solution.

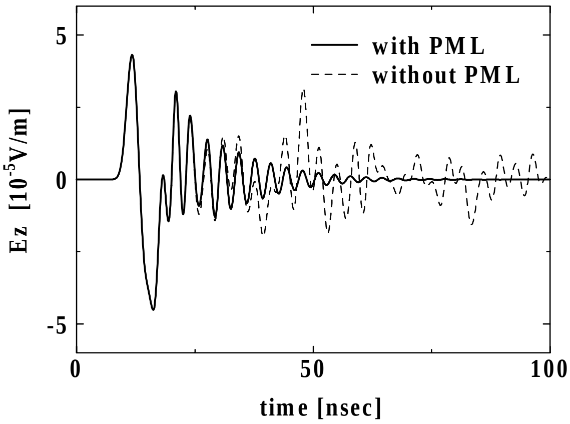

Figure 4: Time response at the interface.

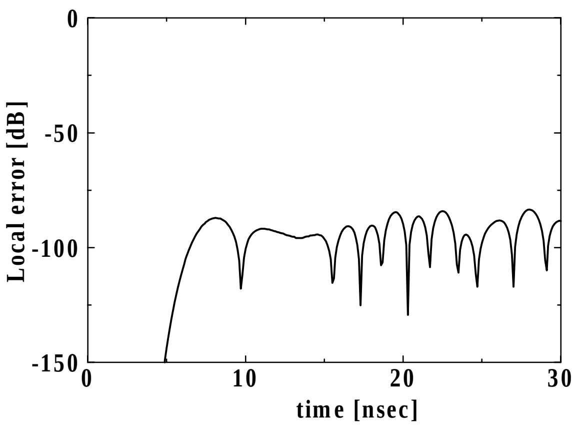

Figure 5: Local error at the interface.